

TEXTURE FEATURE FOR ANALYSIS OF COVID – 19 X-RAY IMAGES

JHARNA MAJUMDAR¹, SHILPA ANKALAKI², GAGAN KARTHIK³,
THRIBHUVAN GUPTA S⁴, SRINATH RAMACHANDRAN⁵, ADITHYA V AMBERKAR⁶,
DARSHAN S SALIMATH⁷, S ROSHAN SAMEER⁸, SHREYAN P SHETTY⁹

¹ Dean R & D, Prof., Dept. of M. Tech CSE, Head, Centre for Robotics Research, Head, Centre for Space Research

² Assistant Prof., Dept. of M. Tech CSE

^{3,4,5,6,7,8,9} Students, Nitte Meenakshi Institute of Technology

¹jharna.majumdar@nmit.ac.in, ²shilpaa336@gmail.com

ABSTRACT:

Medical images perform a significant part in the disease diagnosis and treatment which involves plenty of important medical information. The manual annotation of the images is not efficient approach for handling huge volumes of medical imaging data. This paper focuses on the experimental study on a set of features well suited for analysis of COVID19 X-ray images. This study includes the texture based features like Grey Level Co-occurrence (GLCM), Texture Spectrum, Local Binary Pattern (LBP) and features based on Intensity Histogram like Histogram of Oriented Gradients (HOG). This work aims to provide an overview of the state of the art of texture features for analysis of COVID19 X-rays images. Random Forest and Naïve Bayesian classifiers are employed to classify images into COVID19 and Non COVID19 images.

KEYWORDS: COVID19, Grey Level Co-occurrence Matrix, Texture Spectrum, Local Binary Pattern and Histogram Oriented Gradients

I. INTRODUCTION

COVID-19 has been spreading rapidly into all over countries in the world until it was classified as a pandemic by the World Health Organization (WHO). COVID19 can be diagnosed by performing a blood test, computed tomography, and chest X-ray images. Chest X-ray and Computed tomography (CT) scans are the general image diagnosis approaches for pneumonia detection. The former approach usually results in high misdiagnosis rates compared to the CT scan diagnosis approach. But still, X-ray based diagnosis more popular than CT diagnosis because it is faster, low-cost, expose less radiation to the patients [1-2]. The symptoms of COVID19 are similar to viral pneumonia which can lead to an invalid diagnosis. Subsequently, an incorrect diagnosis may lead to the false labeling of the Non-COVID viral pneumonia as suspicious COVID19 [3]. Many researchers proposed AI/Deep learning-based approaches for COVID19 detection. Some of such works are summarised in this section..

Researchers of [4], proposed an approach for the detection of COVID19 in an early stage. Researchers accomplished this task by employing texture features such as GLCM, LDP, GLRLM, GLSZM, and DWT algorithms. These features are trained using a support vector machine and achieved an accuracy of 99.68%. LBP transform has been applied to the Chest x-ray image and extracted the global texture feature, HOG and uniform LBP features from the LBP transformed image. SVM is used as a classifier to train these features. In this study, researchers employed the SVM as a binary class (Covid19 vs. Normal), Multi-class (Covid19 vs. Viral Infection & Bacteria, and Covid19 vs. Normal, Viral Infection & Bacteria) [5]. Covid19 image retrieval system developed by [6] using handcrafted features (color, texture, and shape) and multi-layer CNN features.

Covid19 X-ray images are classified using the shrunken features [7]. GLCM, LBGLCM, GLRLM, and Segmentation-based Fractal Texture Analysis (SFTA) texture features are extracted and data oversampling has performed using Synthetic Minority Over-sampling Technique (SMOTE). Significant features are extracted using principal component analysis. These shrunken features are trained by the support vector machine.

SegNet Encoder and Decoder architecture is utilized for Covid19 detection [8]. The encoder consists of two streams, one for texture and another for a structural component. The feature map is formed by merging these 2 components. The decoder block performs the operation of unsampling and classification.

Researchers [9] proposed a machine learning approach for distinguishing general pneumonia from coronavirus pneumonia. The dataset was created by taking chest CT images of 73 Covid19 positives patients and 27 confirmed normal pneumonia patients from Ruian People’s Hospital. ROI of the CT image is extracted based on the ground glass opacities (GGOs) and 34 statistical textures are extracted followed by the feature selection using the ReliefF algorithm. These features are trained by using an ensemble of bagged tree (EBT) and other ML classifiers including KNN, Logistic Regression, decision tree and support vector machine using 10-fold cross-validation.

The approach of differentiating influenza pneumonia from novel coronavirus pneumonia was accomplished using deep learning model [10]. CT images are used in this work. Patient data collection followed by the manual lesion region annotation by 2 radiologists. The classification has performed in two ways: lesion level classification is accomplished by VGGNet architecture. Patient-level classification is dependent on lesion level classification which is computed by taking the summation of the predicted probabilities for all the lesions of a patient and then normalized between novel coronavirus pneumonia and Influenza Pneumonia.

II. ALGORITHMS AND METHODOLOGY

The proposed work includes the comprehensive study of texture and other features to determine well suited features to study and analyse the COVID19 and Non COVID19 Images. Fig. 1 describes the methodology adopted in this work. This study has considered 50 COVID19 and 50 Non COVID19 images. Images are pre-processed and divided into 7x7 non overlapping regions for the purpose of local feature extraction. The features extracted for this study are explained in subsequent sections.

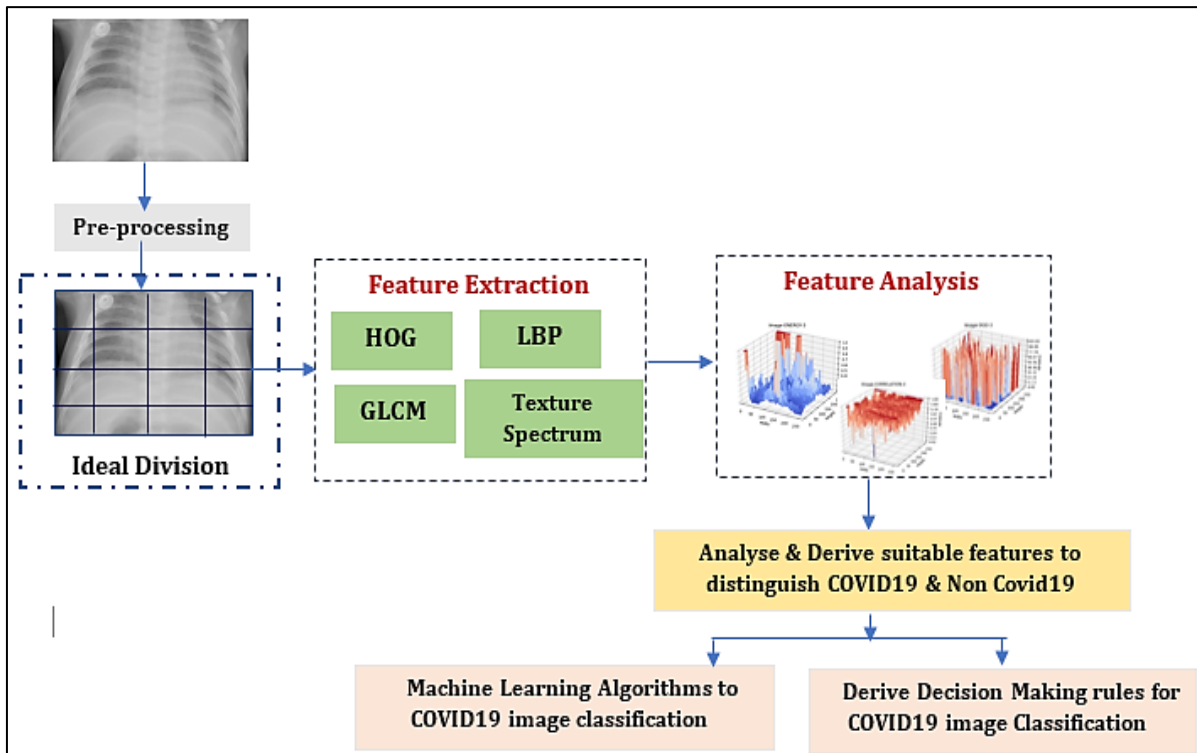


Fig. 1 Proposed Methodology

2.1 Features based on Intensity Histogram (HOG)

Histogram of Oriented Gradients (HOG) [11], is a feature descriptor, which represents the information of image data in the form of features. Fig. 2 depicts the steps involved in the extraction of HOG Features.

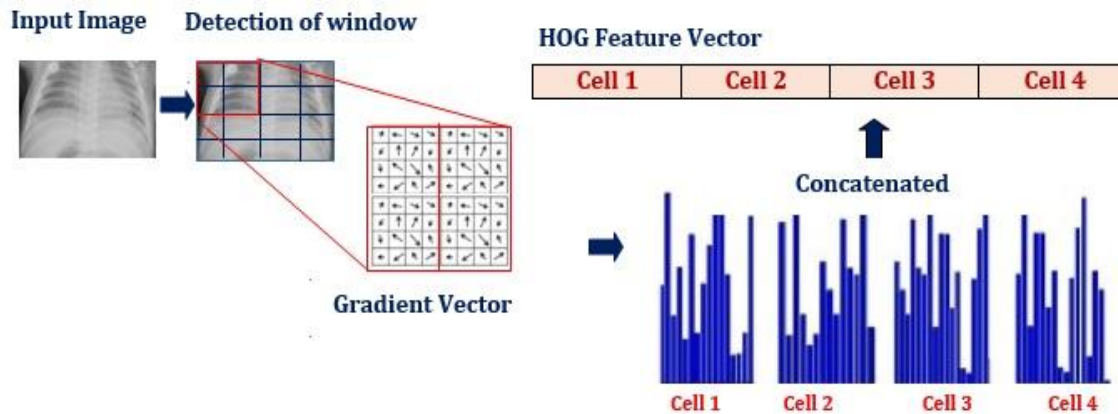


Fig. 2 Steps involved in Histogram of Oriented Gradients

The input image is divided into (NXN) pixel areas called cells. The HOG feature descriptor is dependent on the collection of gradients directions over each pixel of a cell. For every cell, the histogram of gradient directions is computed for individual pixels within the cell. According to the gradient orientation, every cell is discretized into angular bins. The weighted gradient is computed by considering the contribution of each cell's pixel to its analogous angular bin. These cells further clustered into overlapping blocks. These blocks are then normalized to obtain results with optimized illumination invariance. The set of these block histograms represents the descriptor.

2.2 Features based on Texture

Texture is a pattern which has both randomness and regularity. Texture of an image is characterised as distribution of spatial information of intensity levels in neighbouring pixels. The analysis of texture in images provides an important cue for a variety of applications.

Images are best characterized by different texture methods. In this paper, we have used texture to see the variations of COVID-19 across the image. Combining data from different methods and using some form of feature selection can improve the overall texture recognition performance.

2.2.1 Grey Level Co-occurrence Matrix (GLCM) Method [12 - 16]

Texture can be characterized by the spatial interaction among neighbouring pixels. One way to bring this information into the texture analysis process is to consider not only the distribution of intensities, but also positions of pixel with these intensities. Co-occurrence matrices are such matrices, which computes the frequency of pairs of pixels with a particular grey level occurs in a specific spatial relation to another grey level.

It is essentially a 2-D Histogram of frequency of pair of intensity values occur in a specified spatial relationship.

Haralick's texture features based on GLCM: The texture measurement can be calculated using co-occurrence matrix. It is defined as a function of a particular direction and distance, or a function of displacement (dx, dy) along the x and y direction in the image. It is a spatial relationship between two pixels. For a given displacement (dx, dy), the (i, j) element of the co-occurrence matrix is frequency of the grey value at current position (x, y) is i when the value at distant position (x+dx, y+dy) is j. $C^{dx,dy}(i, j) = P(G(x, y) = i \text{ and } G(x+dx, y+dy) = j)$

Computation of the co-occurrence matrix can be performed on the entire image. Though, by computing it in a small window scanning the image, a co-occurrence matrix can be accompanying with every image position.

The size of the co-occurrence matrix is depended on the number of distinct intensities in the input image. Requantization of the given image intensity levels into the fewer grey levels is an approach to obtain the co-occurrence matrix with manageable size.

The six primitive texture features are

- Angular Second Moment (f_1):
$$f_1 = \sum_{i,j=0}^{N-1} P_d^2(i, j)$$

- Contrast (f_2):
$$f_2 = \sum_{i,j=0}^{N-1} (i-j)^2 P_d(i, j)$$
- Maximum Probability (f_3):
$$f_3 = \max(P_d(i, j))$$
- Entropy (f_4):
$$f_4 = \sum_{i,j=0}^{N-1} -P_d(i, j) \times \ln(P_d(i, j))$$
- Homogeneity (f_5):
$$f_5 = \sum_{i,j=0}^{N-1} \frac{P_d(i, j)}{1 + (i-j)^2}$$
- Variance (f_6):
$$f_6 = \frac{1}{N^2} \sum_{i,j=0}^{N-1} (i-\mu_i) \times (j-\mu_j) \times P_d(i, j)$$

Where,

$$\mu_i = \sum_{i,j=0}^{N-1} i \times P_d(i, j) \quad \text{and} \quad \mu_j = \sum_{i,j=0}^{N-1} j \times P_d(i, j)$$

Since the size of the co-occurrence matrix depends on the number of grey levels, it takes more time for calculation if the number of grey levels is high. Hence requantization to reduce the number of grey levels in the input image is a prerequisite.

Texture Spectrum (TS) Method [17 – 19]

Texture Spectrum is a frequency plot of the texture units in a grey scale plot. He and Wang developed the texture unit as follows. Texture unit can be computed for a given pixel by comparing it with its eight neighbourhood pixels. The texture unit, TU, is the set of E_i ($i = 1, 2, \dots, 8$) where:

$$E_i = \begin{cases} 0, & \text{if } V_i < V_0 \\ 1, & \text{if } V_i = V_0 \\ 2, & \text{if } V_i > V_0. \end{cases}$$

V_1	V_2	V_3
V_8	V_0	V_4
V_7	V_6	V_5

Fig. 3: Labelling of neighbourhood pixels.

Fig.3 shows the ordering of pixels used for the calculation. The texture unit number is then calculated using the following formula:

$$N_{TU} = \sum_{i=1}^8 E_i 3^{i-1}$$

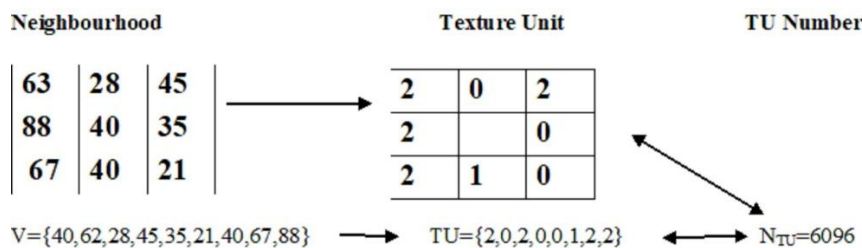


Fig. 4 Example of determining the texture unit number from a neighbourhood of pixels

Fig.4 shows an example of how the texture unit number is determined from an input pixel and its neighbourhood. In this manner, each pixel in an image can be labelled with a specific texture unit number, N_{TU} . The texture spectrum, $S(i)$, is simply the frequency distribution of these texture units. Not only do He and Wang suggest using the sum of absolute differences as a distance measure between two texture spectra, but they also suggest that certain texture features can be calculated from texture spectra:

$$\text{Black-White Symmetry} = \left[1 - \frac{\sum_{i=0}^{3279} |S(i) - S(3281 + i)|}{\sum_{i=0}^{6560} S(i)} \right] \times 100$$

$$\text{Geometric Symmetry} = \left[1 - \frac{1}{4} \sum_{j=1}^4 \frac{\sum_{i=0}^{6560} |S_j(i) - S_{j+4}(i)|}{2 \times \sum_{i=0}^{6560} S_j(i)} \right] \times 100$$

$$\text{Degree of Direction} = \left[1 - \frac{1}{6} \sum_{m=1}^3 \sum_{n=m+1}^4 \frac{\sum_{i=0}^{6560} |S_m(i) - S_n(i)|}{2 \times \sum_{i=0}^{6560} S_m(i)} \right] \times 100.$$

They then go on to suggest a number of oriented texture features: the micro-horizontal structure (MHS), the micro-vertical structure (MVS) and two micro-diagonal structures (MDS1, MDS2):

$$\begin{aligned} \text{MHS} &= \sum_{i=0}^{6560} S(i) \times \text{HM}(i) & \text{HM}(i) &= P(E_1, E_2, E_3) \times P(E_5, E_6, E_7) \\ \text{MVS} &= \sum_{i=0}^{6560} S(i) \times \text{VM}(i) & \text{VM}(i) &= P(E_1, E_5, E_7) \times P(E_3, E_4, E_5) \\ \text{MDS1} &= \sum_{i=0}^{6560} S(i) \times \text{DM1}(i) & \text{DM1}(i) &= P(E_1, E_2, E_5) \times P(E_4, E_5, E_6) \\ \text{MDS2} &= \sum_{i=0}^{6560} S(i) \times \text{DM2}(i), & \text{DM2}(i) &= P(E_2, E_3, E_4) \times P(E_6, E_7, E_8) \end{aligned}$$

Where, $P(E_a, E_b, E_c)$ represents the number of elements in $\{E_a, E_b, E_c\}$ which have the same value for texture unit i .

Finally, they propose the central symmetry feature:

$$\text{Central Symmetry} = \sum_{i=0}^{6560} S(i) \times K(i)^2$$

Where $K(i)$ is the number of pairs having the same values in the elements:

(E_1, E_5) , (E_2, E_6) , (E_3, E_7) and (E_4, E_8) for texture unit i .

2.2 Local Binary Pattern (LBP) [21 - 22]

Local Binary Pattern [17-18] is one of simplest and powerful local descriptor. It is a specific case of the Texture Spectrum model. The binary code is generated for every pixel in an image using a simple comparison. The value of the central pixel will be encoded as 1 if value of the centre pixel is greater than neighbouring pixels otherwise 0. In the same way a binary pattern is calculated for the entire image to get the LBP image.

$$B_i = \begin{cases} 0 & \text{if } P_i < P_0 \\ 1 & \text{if } P_i > P_0 \end{cases}$$

Where B_i denotes the elements of the binary pattern formed for $i = \{1,2,3,\dots,8\}$. Each element B_i occupies the same position as that of pixel i . Follow the pixel along the clockwise or anti-clockwise to get the binary pattern.

2.3 Gaussian Naïve Bayesian classification [20, 23]

In this study, Naïve Bayesian classification employed for the purpose of classification of COVID19 and Non COVID 19 images. The texture and other local features extracted from the images are analysed and determined the well suited features and these features are used as input to the classifier. The working principle of Gaussian Naïve Bayesian is as follows:

Step 1: Create the training dataset with labelling samples that is the pair of set of attributes along with its class label. In this case the dataset consists of 2 classes that is COVID and Non COVID

Step2: Compute the probability using Bayesian theorem

$$P(C_i|X) = \frac{P(X|C_i)P(C_i)}{P(X)}$$

Where $P(X)$ probability of data independent to the classes. Usually $P(X)$ is equal for all classes. $P(C_i)$ is the prior probability of class. Usually we assume a uniform distribution for all classes. $P(C_i|X)$ and $P(X|C_i)$ posterior probabilities. The $P(C_i|X)$ is maximized when $P(X|C_i)P(C_i)$ is maximized.

Step 3: The input attribute values considered in this work are continuous hence the Gaussian distribution is well suited in this case. The Gaussian distribution formula is as follows:

$$g(x, \mu, \sigma) = \frac{1}{\sqrt{2\pi}\sigma} e^{-\frac{(x-\mu)^2}{2\sigma^2}}$$

Where μ and σ are mean and standard deviation respectively. This can be used to compute $P(x_k|C_i) = g(x_k, \mu_{C_i}, \sigma_{C_i})$

2.4 Random Forest Classifier (RF Classifier) [24]

RF classifier [20] is supervised algorithm that is made up of cluster of multiple trees which results to robust trees. The initial step of the algorithm is to select the sample data points randomly from the dataset. For every sample data, the decision tree will be constructed and collects the prediction results of each tree. In further step, the results of all decision tree will be collected and perform the voting for every prediction result. The final decision will be taken based on the prediction result which got maximum votes.

III. RESULTS AND ANALYSIS

In this work, Local Binary Pattern (LBP), Histogram Oriented Gradients (HOG), Grey Level Co-occurrence Matrix Method and Texture Spectrum features are extracted locally by using 7x7 non overlapping window. Fig.3 illustrates the GLCM features and its respective histogram for COVID19 image and Fig.4 illustrates the HoG features and its respective histogram for Non COVID19 image.

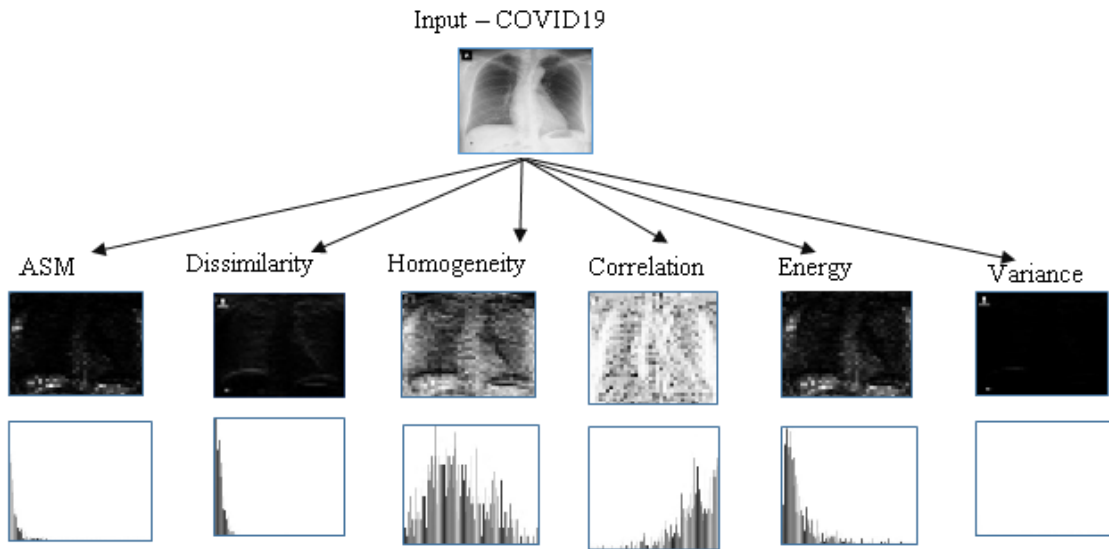


Fig. 5 GLCM features and histograms for COVID19 image

From the experiment conducted on 50 COVID19 and 50 Non COVID19 images, the histogram characteristics of each feature image. The sample histograms are depicted in Fig.5 and 6. After analysing the histogram characteristics of all COVID images with respect to each feature, we derived the generalised characteristics of COVID19 images. Same procedure is repeated with non COVID19 images to illustrate its histogram characteristics. The sample histogram of all features for Non COVID19 image is depicted in Fig. 7 and 8. The purpose of plotting the histogram is to analyse images with respect to the texture distribution. The histogram characteristics like brightness, contrast, entropy, spatial frequency and visibility are extracted for each feature image, feature are tabulated and analysed for further process.

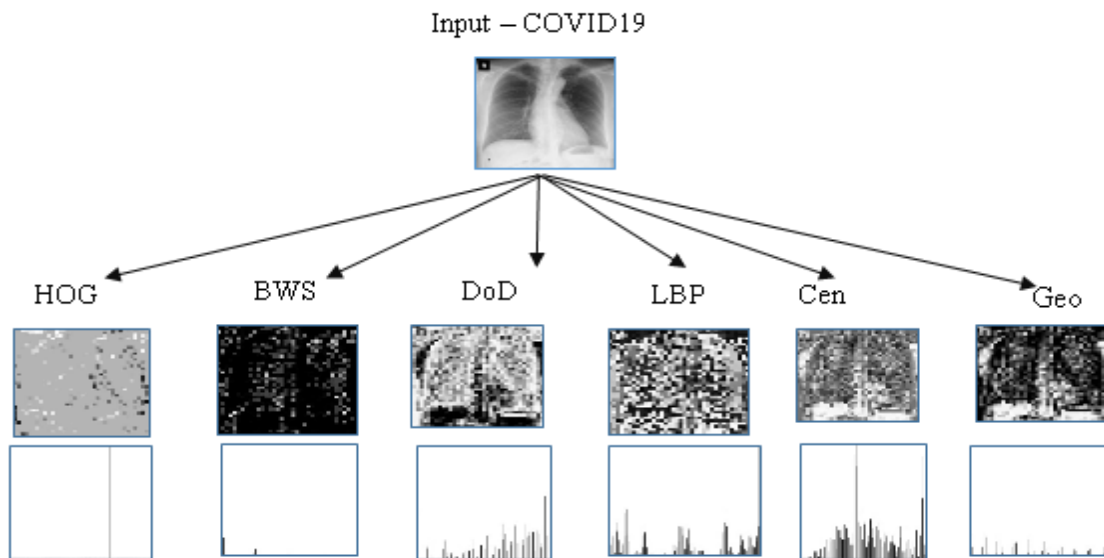


Fig. 6 HOG, LBP and Texture features and histograms for COVID19 image.

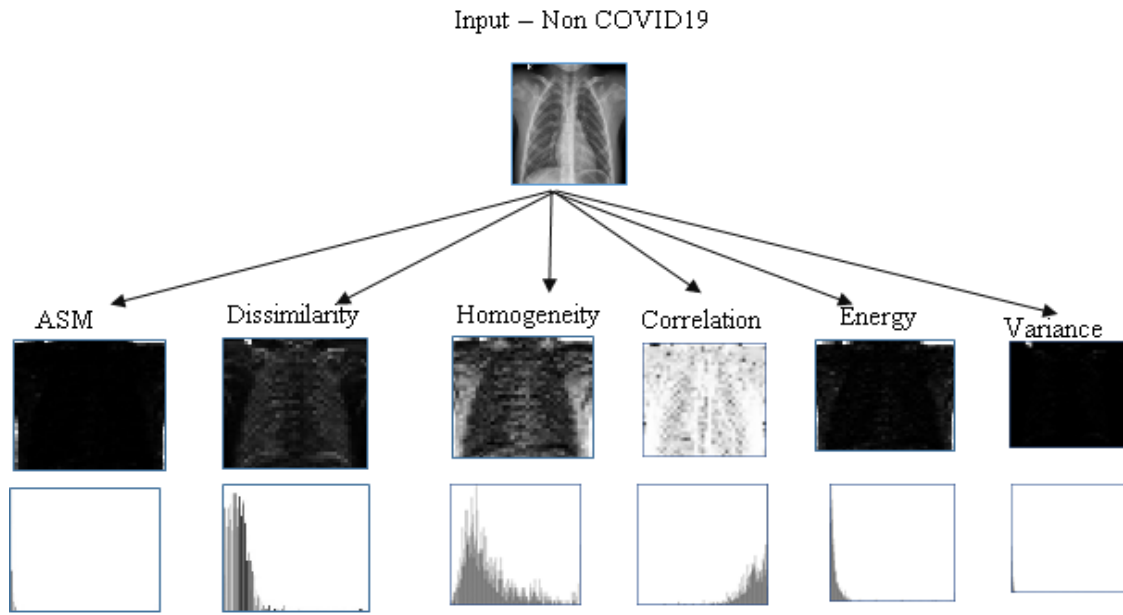


Fig. 7 GLCM features and histograms for COVID19 image

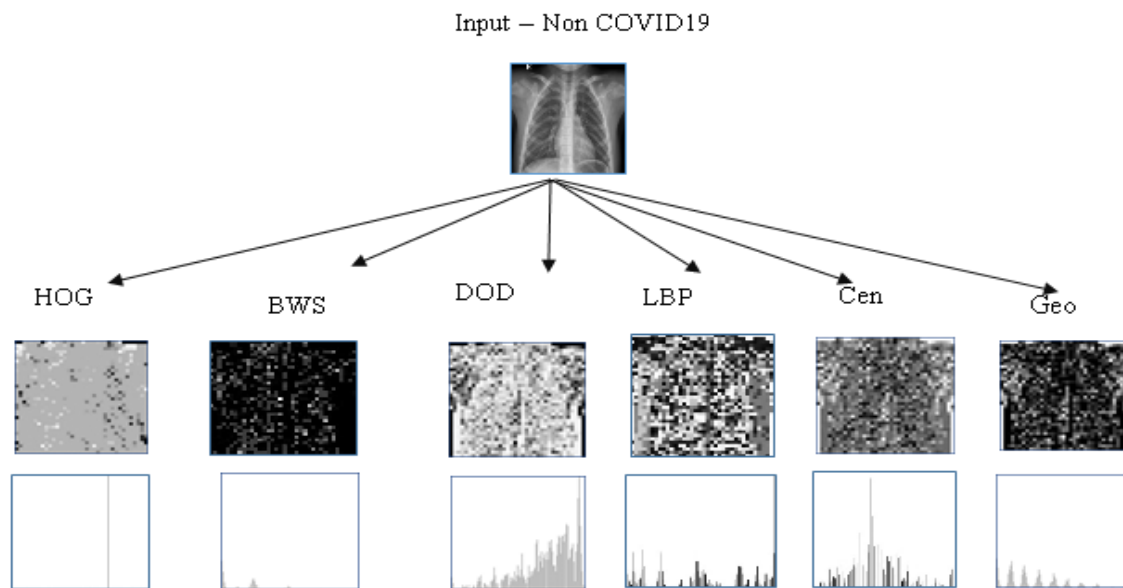


Fig. 8 HOG, LBP and Texture features and histograms for COVID19 image.

The features of ASM, Correlation, Variance, HOG, BWS, LBP, Cen and Geo are having the narrow histograms and identical for COVID19 and Non COVID19 images. The histograms of dissimilarity, homogeneity, energy and Degree of Directivity (DoD) feature images are wider in range and unique for both COVID19 and Non COVID19 images. The analysis derived from the histogram characteristics are as follows:

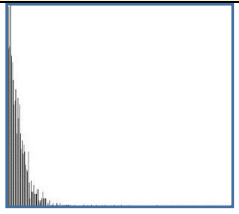
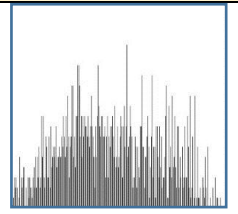
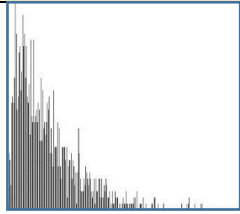
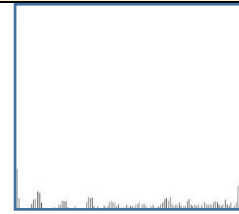
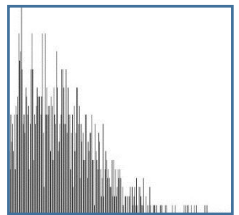
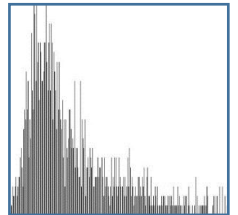
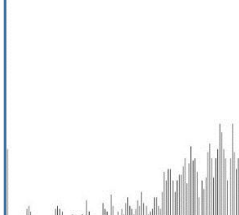
Dissimilarity: The dissimilarity histogram of COVID19 images are having the peaks more towards the lower values whereas dissimilarity histogram for non COVID19 images consist of broad range of peaks distributed throughout the histogram axis.

Homogeneity: The pixel distribution is throughout the axis which represents the higher contrast for COVID image and pixel distribution and more number of peaks located towards the darker region of the histogram.

Energy: The Histogram distribution shifts from brighter region to darker region when we move from COVID19 to Healthy images.

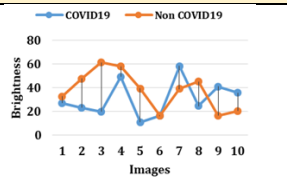
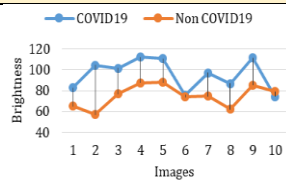
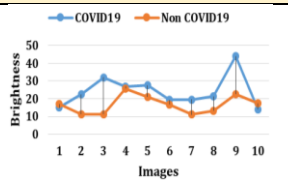
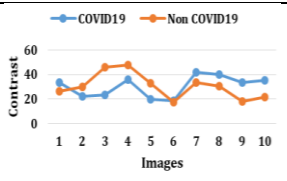
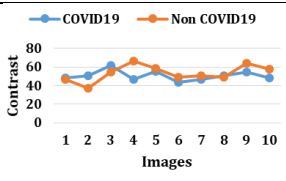
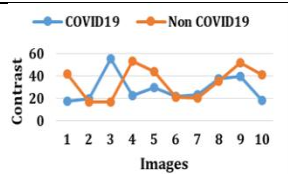
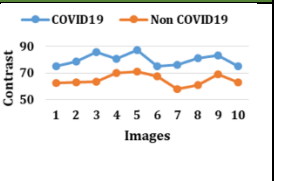
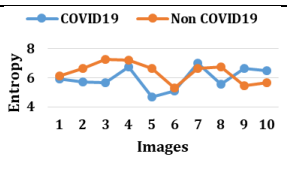
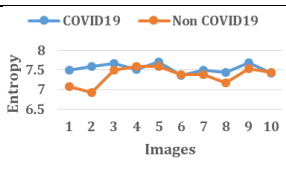
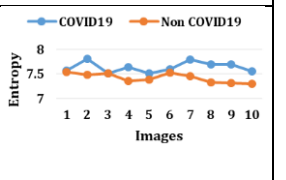
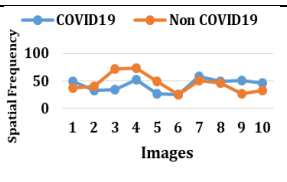
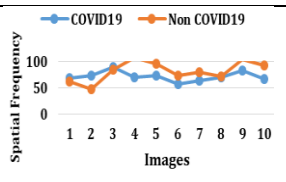
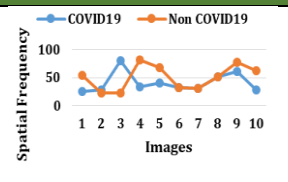
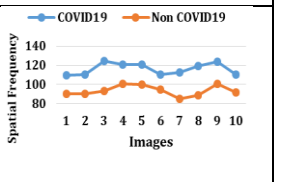
Degree of Directivity (DoD): Pixel distribution increases on the brighter region when we move from COVID affected to Healthy image. That is, a greater number of pixels are distributed in the brighter region when we move from Covid19 affected to Healthy image. All these histograms are depicted in Table 1.

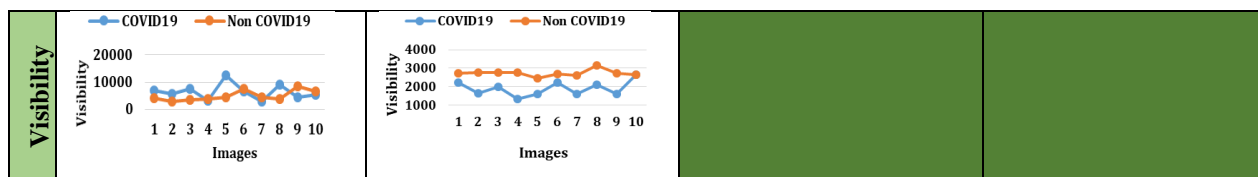
Table 1: Histogram images of COVID19 and Non COVID19 images

Image	Dissimilarity	Homogeneity	Energy	Degree of Directivity (DoD)
COVID 19				
Non COVID 19				

The histogram characteristics also studied for dissimilarity, homogeneity, energy, variance and DOD.

Table 2: Histogram Characteristics analysis for Texture features for COVID19 and Non COVID19 images

	Feature Image			
	Dissimilarity	Homogeneity	Energy	DOD
Brightness				
Contrast				
Entropy				
Spatial Frequency				



The analysis shown in the Table 2, depicts that Brightness and Visibility characteristics of the DOD feature images varies from COVID19 to Non COVID images. The brightness value of DOD feature images of COVID19 are in the range of 118-143 and Non COVID19 images are in the range of 170-184. Similarly the visibility of DOD image for COVID19 is in the range of 1294-2387 and for non COVID19 images in in the range of 848-1016 respectively. Entropy and Visibility of the energy features have distinct ranges for COVID19 and Non COVID19 images. The range of entropy of energy feature for COVID19 images is 5-7 whereas for Non COVID19 images is 4-5. Similarly the visibility of energy feature for COVID19 images is in the range of 4765-8503 and for non COVID19 images in in the range of 10426-16159 respectively. The histogram characteristic of particular feature which distinguishes between COVID19 and Non COVID19 images is represented in the green color block of the Table2. All these analysis are derived using the limited set of COVID19 and Non COVID19 chest X-ray images.

The analysed features are trained using the Naïve Bayesian and Random Forest, and achieved the classification result of 82.56% and 85.714% accuracy respectively to classify COVID19 and Non COVID19 images.

IV. CONCLUSION

This work analysed the texture based features for chest x-ray images by using extracting the local texture features using the 7X7 kernel and all texture generated features are further analysed by extracting the histogram characteristic. In this process, DOD and Energy texture found as good features with respect to its histogram characteristics brightness, entropy and visibility. Machine Learning classifiers Naïve Bayesian and Random forest are trained using these features and obtained the accuracy of 82.56% and 85.714% accuracy respectively to classify the images into COVID19 and Non COVID19 images.

V. ACKNOWLEDGMENT

The authors express their heartfelt thanks to Visvesvaraya Technological University (VTU), Belagavi, Karnataka for providing an opportunity, facility and financial support to carry out this research. The authors express their sincere gratitude to Prof N.R Shetty, Advisor and Dr H.C Nagaraj, Principal, Nitte Meenakshi Institute of Technology for giving constant encouragement and support to carry out research at NMIT.

REFERENCES

1. Geoffrey D Rubin, Christopher J Ryerson, Linda B Haramati, Nicola Sverzellati, Jeffrey P Kanne, Suhail Raof,Neil W Schluger, Annalisa Volpi, Jae-Joon Yim, Ian BK Martin, et al. “The role of chest imaging in patient management during the covid-19 pandemic: a multinational consensus statement” Fleischner society. Chest, 2020.
2. Wesley H. Self, D. Mark Courtney, Candace D. McNaughton, Richard G. Wunderink, and Jeffrey A. Kline. “High discordance of chest x-ray and computed tomography for detection of pulmonary opacities in ed patients: implications for diagnosing pneumonia”, The American journal of emergency medicine, 31(2):401–405, 2013.
3. Ali Mohammad Alqudah, Shoroq Qazan , Amin Alqudah et al. “Automated Systems for Detection of COVID-19 Using Chest X-ray Images and Lightweight Convolutional Neural Networks”, 27 April 2020, PREPRINT (Version 1) available at Research Square [+https://doi.org/10.21203/rs.3.rs-24305/v1+]
4. Barstuğan, Mücahid & Özkaya, Umut & Öztürk, Şaban, “Coronavirus (COVID-19) Classification using CT Images by Machine Learning Methods”,2020
5. Dhurgham Al-Karawi , Shakir Al-Zaidi, Nisreen Polus, Sabah Jassim, “AI based Chest X-Ray (CXR) Scan Texture Analysis Algorithm for Digital Test of COVID-19 Patients”, https://doi.org/10.1101/2020.05.05.20091561
6. Vijayakumar Bhandi, Sumithra Devi. K. A, “COVID-19 X-ray Image Retrieval Using Deep Convolutional Neural Networks”, American Journal of Engineering Research (AJER) e-ISSN: 2320-0847 p-ISSN : 2320-0936 Volume-9, Issue-7, pp-47-55
7. Saban Ozturk , Umut Ozkaya, Mucahid Barstugan, “Classification of Coronavirus Images using Shrunken Features”, doi: <https://doi.org/10.1101/2020.04.03.20048868>

8. Omar Elharrouss, Noor Almaadeeda, Nandhini Subramaniana, Somaya Al-Maadeeda, “An encoder-decoder-based method for COVID-19 lung infection segmentation”, arXiv:2007.00861v2 [eess.IV] 4 Jul 2020
9. Chenglong Liu, Xiaoyang Wang, Chenbin Liu et al. “Differentiating novel coronavirus pneumonia from general pneumonia based on machine learning”, 02 July 2020, PREPRINT (Version 2) available at Research Square [+https://doi.org/10.21203/rs.3.rs-31313/v2+]
10. Zhou, Min & Chen, Yong & Wang, Dexiang & Xu, Yanping & Yao, Weiwu & Huang, Jingwen & Jin, Xiaoyan & Pan, Zilai & Tan, Jingwen & Wang, Lan & Xia, Yihan & Zou, Longkuan & Xu, Xin & Wei, Jingqi & Guan, Mingxin & Feng, Jianxing & Zhang, Huan & Qu, Jieming. “Improved deep learning model for differentiating novel coronavirus pneumonia and influenza pneumonia”, 2020, 10.1101/2020.03.24.20043117.
11. N. Dalal and B. Triggs, “Histograms of oriented gradients for human detection” in Computer Vision and Pattern Recognition, 2005. CVPR 2005. IEEE Computer Society Conference on, 2005.
12. Haralick et al., “Textural Features for Image Classification”, IEEE Transaction on Systems, Man and Cybernetics”, Vol. SMC-3, No.6, November 1973, pp. 610-621
13. Jharna Majumdar and Bhuvaneshwari S. Patil, “A Comparative Analysis of Image Fusion Methods Using Texture” Proceedings of the Fourth International Conference on Signal and Image Processing 2012 (ICSIP 2012), Lecture Notes in Electrical Engineering 221, DOI: 10.1007/978-81-322-0997-3_31, Springer India 2013
14. Priya Ronad, Shilpa Ankalaki, Jharna Majumdar, “Texture and Color Features for Animal Identification” International Journal of Computer & Mathematical Sciences (IJCMS-15), ISSN 2347 – 8527, Volume 4, Issue 9, September-2015.
15. Priyanka A R, Jharna Majumdar, “Video Shot Detection using Texture Feature” International Journal of Science and Research (IJSR), ISSN (Online): 2319-7064, Volume 4 Issue 8, August 2015.
16. Jharna Majumdar, MP Ashray, Madhan HM, Dhanush M Adiga “Video Shot Detection and Summarization Using Features Derived From Texture”, International Conference on Cybernetics, Cognition and Machine Learning Applications (ICCCMLA) – 2019 on 16–17 August 2019 at Goa and published in the Springer Studies in Computational Intelligence, Online ISBN 978-981-15-1632-0, pp 163-175, April 2020 (Indexed in SCOPUS , DBLP, UGC ,SpringerLink & Major AI)
17. Karkanis, Stavros & Galousi, K. & Maroulis, Dimitris. “Classification of Endoscopic Images Based on Texture Spectrum”. ACAI99, Workshop on Machine Learning in Medical Applications.2000
18. DC. He and L. Wang, "Texture Unit, Texture Spectrum, And Texture Analysis", Geoscience and Remote Sensing, IEEE Transactions, 1990, vol. 28, pp. 509 - 512.
19. H. Sarojadevi, Jharna Majumdar, “Artificial Neural Network based Classification of Micro Air Vehicle Images”, International Journal of Computer Application, Issue 2, Volume 3 (June 2012) ISSN: 2250-1797, pp. 411 – 418
20. Shilpa Ankalaki, Laxmidevi Noolvi, Jharna Majumdar, “Leaf Identification Based on Fuzzy C Means and Naïve Bayesian Classification” International Journal of Advanced Research In Engineering And Technology (IJARET) ISSN 0976 - 6499 (Online) Volume 5, Issue 7, pp. 71-82, July 2014.
21. Turker Tuncer, Sengul Dogan, Fatih Ozyurt, “An automated Residual Exemplar Local Binary Pattern and iterative ReliefF based COVID-19 detection method using chest X-ray image” ,Chemometrics and Intelligent Laboratory Systems, Volume 203, 2020, 104054, ISSN 0169-7439, https://doi.org/10.1016/j.chemolab.2020.104054.
22. Jharna Majumdar, Dhanush M Adiga, Madhan HM, MP Ashray “Comparison of Video Shot Detection Methods Using Higher Order Local Descriptor” International Conference on Advanced Informatics for Computing Research (ICAICR) 2019, Shimla, July 15-16, 2019 and published in the proceedings of the ICAICR 2019, ACM New York, NY, USA ©2019 DOI: .org/10.1145/3339311.3339324, ISBN: 978-1-4503-6652-6
23. Nafizatus Salmi and Zuherman Rustam, “Naïve Bayes Classifier Models for Predicting the Colon Cancer”, IOP Conf. Series: Materials Science and Engineering 546 (2019) 052068 doi:10.1088/1757-899X/546/5/052068
25. Md. Zahangir Alam, M. Saifur Rahman, M. Sohel Rahman, “A Random Forest based predictor for medical data classification using feature ranking”, Informatics in Medicine Unlocked, Volume 15, 2019, 100180, ISSN 2352-9148, https://doi.org/10.1016/j.imu.2019.100180.